Monolithic Silicon Light Sources

Philippe M. Fauchet

Department of Electrical and Computer Engineering, University of Rochester
Rochester NY 14627-0231, USA
fauchet@ece.rochester.edu

Abstract. Monolithic silicon light sources (LEDs and lasers) could have a significant impact when integrated on silicon chips. After a general introduction to light emission in silicon, this chapter discusses the mechanisms of light emission in bulk silicon, silicon quantum dots, silicon alloyed with germanium, and silicon doped with specific impurities such as erbium. Then, the fabrication and performance of LEDs using these materials are discussed. The chapter ends with a discussion of the prospects for a silicon laser.

1 Introduction

Light emission occurs when an electron recombines with a hole to produce a photon. The photon energy is equal to the band-gap energy if the electron is in the conduction band and the hole in the valence band. If both electron and hole are located at the same point in the Brillouin zone, the radiative recombination rate is large and the radiative lifetime τ_{rad} is short (typically a few ns). This is the case in direct gap semiconductors, such as GaAs. In indirect gap semiconductors such as Si, the bottom of the conduction band is not at the same location in reciprocal space as the top of the valence band. Radiative recombination across the band-gap thus requires the participation of a phonon, making it a second-order process. As a result, the radiative lifetime is much longer, typically in the msec regime.

The internal quantum efficiency is given by

$$\eta_{\text{in}} = \frac{\tau_{\text{non-rad}}}{\tau_{\text{non-rad}} + \tau_{\text{rad}}} \tag{1}$$

where $\tau_{\text{non-rad}}$ is the lifetime for the recombination pathways that do not involve the production of photons. Non-radiative pathways include recombination at bulk or surface defects and Auger recombination. In direct gap semiconductors, η_{in} can be very large, typically of the order of 10% and may even approach 100%, because the radiative lifetime can be shorter than the non-radiative lifetime [1]. However, in indirect gap semiconductors such as Si, the non-radiative lifetime is usually much shorter than the radiative lifetime and η drops by several orders of magnitude and typically is as low as 10^{-4}% to 10^{-5}%.

Several approaches have been proposed to improve the quantum efficiency of silicon. These approaches can be grouped into two categories. In the first

L. Pavesi, D. J. Lockwood (Eds.): Silicon Photonics, Topics Appl. Phys. **94**, 177–199 (2004)

category, non-radiative recombination pathways are suppressed. To achieve this goal, bulk and surface defects must be eliminated. In bulk silicon, this can be done by carefully passivating the surface [2] and by using high purity material [3]. In addition, the injected carrier concentration must remain low to eliminate Auger recombination, as the Auger rate increases with the third power of the injected carrier density [4]. In the second category, the radiative recombination rate is enhanced. This can be achieved by localizing the electron and hole wavefunctions in the same region of space, for example using quantum dots [5] or isoelectronic impurities [6].

Other possibilities include combining silicon with another elemental semiconductor and using specific light emitting centers. Alloying is typically done with germanium [7], although alloys of Si with C and Ge have also shown promise [8]. Silicon-germanium quantum wells superlattices have been successfully employed to achieve luminescence below the band-gap energy of silicon [9]. Transfer of an electron and a hole from silicon to a specific center can lead to efficient sub-band-gap luminescence. Erbium is by far the most widely used light emitting center in bulk silicon [10] as well as in nanocrystalline silicon [11].

Multiple studies of the photoluminescence (PL), especially its origin, in all these forms of silicon have been published. Very high PL efficiencies have been reported. However, light emitting devices must be driven by current and achieving efficient electroluminescence (EL) has proven more challenging. We need to distinguish three efficiencies: the internal quantum efficiency η_{in}, the external quantum efficiency η_{ext}, and the power efficiency η_{p}. The internal quantum efficiency expresses the potential for light emission. It is defined as the fraction of electron–hole pairs that recombine radiatively (see (1)). The external quantum efficiency takes into account the fact that not all the photons generated inside the structure can be detected outside it. For example, total internal reflection prevents photons emitted at an angle to the sample surface from escaping. This is especially a problem when the index of refraction is large, as the fraction of the light that can escape is approximately given by $1/2n^2$ [12]. Solutions to this problem include texturing the surface [3], adding an antireflection coating [13], or decreasing the average index of refraction by using silicon oxide instead of silicon. In addition, in a device structure, the internally emitted photons may be partially absorbed in heavily doped region or at metal contacts. Note that both the internal quantum efficiency and the external quantum efficiency can be measured in PL and EL experiments. Finally, the power efficiency is defined as the ratio of the output light power over the input electrical power. This is the most important quantity for evaluating how useful an LED might be. In most cases, it can simply be obtained by multiplying η_{ext} by the ratio of the emitted photon energy over the applied voltage.

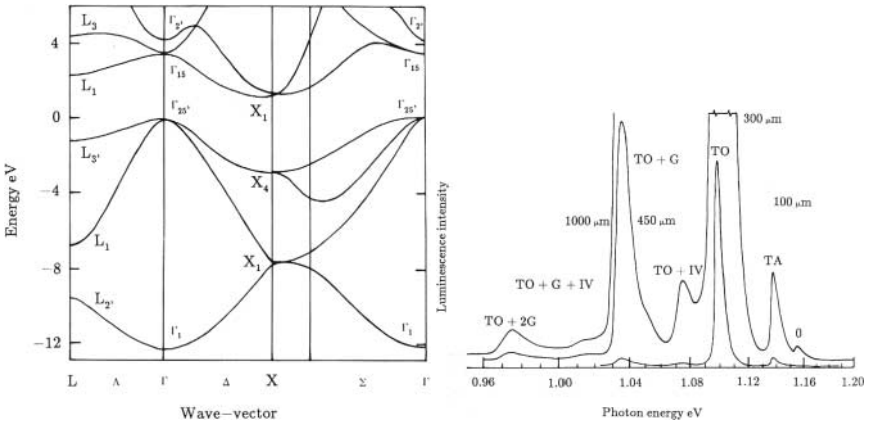

Fig. 1. Silicon band-structure and low-temperature photoluminescence spectrum. Radiative recombination without the participation of a phonon (peak labeled 0) is much weaker than radiative recombination involving at least one phonon. After *Davies* [15]

2 Mechanisms of Silicon Light Emission

Silicon is an indirect band-gap semiconductor [14]. The radiative recombination of an electron near the X-point and a hole at the Γ-point requires the participation of a phonon [15]. This has two major consequences. Because the process is a second order process, the recombination rate is orders of magnitude less than in a typical direct gap semiconductor such as GaAs. In addition, the luminescence lineshape reflects the participation of phonons as illustrated in Fig. 1.

At room temperature, light emission across the band-gap of bulk silicon results from the recombination of a free electron with a free hole. At lower temperatures however, electrons and holes are bound by Coulombic attraction and they form excitons. The volume of space through which an exciton can move before it recombines can be approximated as a sphere whose radius can exceed 100 μm in high quality samples. If this volume contains a non-radiative defect, the exciton recombines without emitting light.

By confining the exciton (or the electron and the hole) in a small volume that is free of defects, it is possible to enhance the quantum efficiency. The most common way to achieve such a confinement is to use small silicon nanocrystals. When the size of the nanocrystal drops below the Bohr exciton diameter ($\sim$ 10 nm), quantum confinement increases the value of the band-gap. Such small objects are called quantum dots. The simplest method to calculate the opening of the band-gap with decreasing size is the effective mass approximation, in which the bands are approximated by parabolas. Because of the complexity of the silicon band-structure however other methods such as tight-binding, pseudopotential, or ab initio local density approxima-

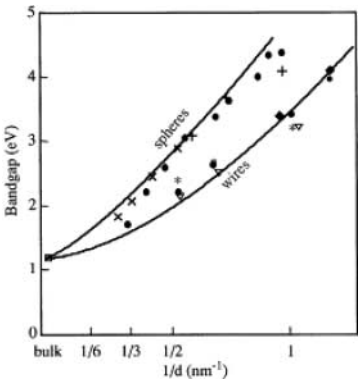

Fig. 2. Silicon quantum dot and quantum wire band-gap versus size calculated using an empirical tight binding approximation (*lines*) and other techniques. The silicon surface is passivated with hydrogen. After *Delerue* [17]

tions must be used to obtain more accurate values [16]. Figure 2 shows the calculated opening of the band-gap, defined as the energy separating the lowest conduction band state from the highest valence band state [17]. The band-gap increases as $d^{-1.3}$, where d is the quantum dot diameter, whereas the effective mass approximation would have predicted a d^{-2} dependence. The localization of the electron and hole wavefunctions in a dot of decreasing size also increases their spread in reciprocal space [5], hence increasing their overlap and the radiative recombination rate. Figure 3 shows how the recombination rate increases with decreasing size/increasing band-gap. Eventually, for very small dots, radiative recombination without participation of phonons should become more likely than radiative recombination involving a phonon. This cross-over is thought to occur for sizes $\leq 2\,\mathrm{nm}$.

Quantum dots have a large surface to volume ratio, with up to 50% of atoms at or near the surface. It is thus not surprising that the quantum dot surface must be well passivated: even one non-radiative recombination center, such as a dangling bond, prevents luminescence (one defect per quantum dot corresponds to an equivalent bulk defect concentration of $\sim 10^{20}\,\mathrm{cm}^{-3}$!). What would happen if the surface contained one center that is capable of producing light? If the states involved in the intra-center recombination are lined up inside the band-gap of the quantum dots, then the electron-hole pair is quickly captured by the center and recombination takes place at the specific energy of the intra-center transition. This is the case with some silicon-oxygen bonds and with erbium. Consider a H-passivated silicon quantum dot. If one Si = O bond forms on its surface, the states associated with this bond appear inside the band-gap provided that the dot size is small enough. Figure 4 shows that when this takes place, the measured luminescence energy increases very slowly and eventually saturates [18]. Further studies have shown that adding more Si = O bonds on the surface does not alter this picture [19].

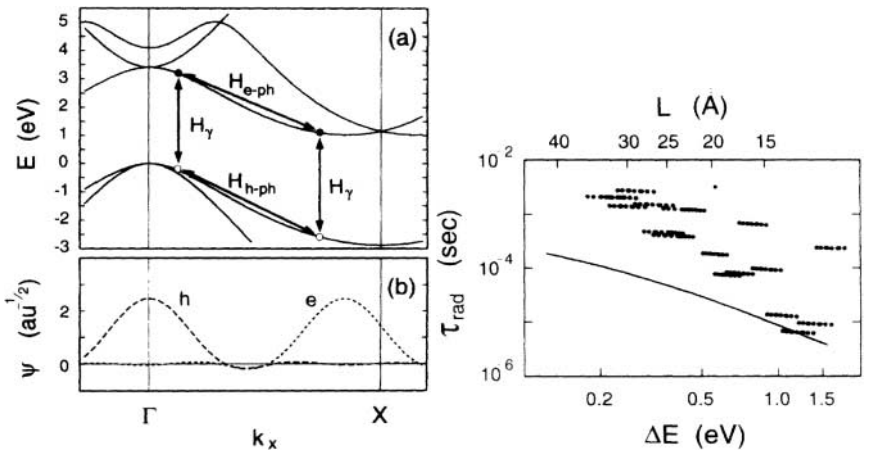

Fig. 3. Spread of the electron and hole wavefunction is a quantum dot and calculated radiative lifetime versus size for silicon quantum dots. The *line* corresponds to phonon-assisted recombination and the points to phonon-less recombination. After *Hybertsen* [5]

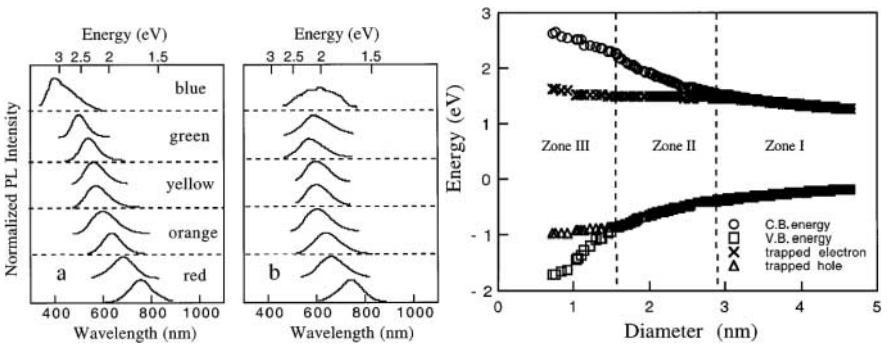

Fig. 4. Measured photoluminescence spectra in various porous silicon samples before exposure to any oxygen (*top left*) and after exposure to oxygen (*top right*). The samples are labeled according to their peak PL wavelength. The average quantum dot size decreases from $\geq 4\,\text{nm}$ (*red*) to $< 2\,\text{nm}$ (*blue*). Calculated conduction band and valence band energy levels for H-passivated Si quantum dots and calculated energy levels associated with a trapped electron and a trapped hole at a Si = O bond at the surface. As the size decreases and the band-gap increases by quantum confinement, the Si = O levels appear inside the band-gap. The expected PL energy difference between H-passivated Si quantum dots and quantum dots containing one Si = O surface bond increases as the size decreases below 2.5 nm to 3 nm, in agreement with the PL spectra. After *Wolkin* [18]

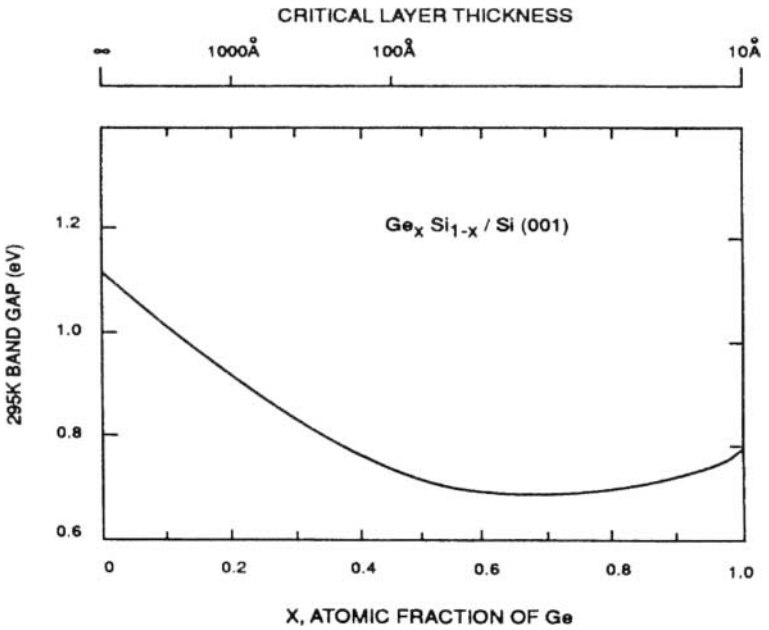

Fig. 5. Calculated band-gap energy for strained SiGe layers grown on silicon. Because the lattice mismatch between Si and the alloy increases with increasing Ge content, the critical thickness above which dislocations occur and strain is relaxed decreases dramatically. After *Pearsall* [22]

When erbium is on the surface or in close proximity to the quantum dot, energy transfer takes place between the quantum dot and erbium, resulting in efficient luminescence near 1.5 μm [20, 21].

Alloying silicon with germanium has also yielded interesting results. One approach consists of using thin (quantum wells) or thick silicon-germanium layers sandwiched between silicon barriers [22]. Luminescence is produced at the band-gap of the alloy, which can in principle be tuned from the band-gap of Si to that of Ge (Fig. 5). Because of the 4% lattice mismatch between Si and Ge, the thickness of the layers must remain small. Another approach, called Brillouin zone folding, is an attempt at modifying the band structure by using alternating layers of Si and Ge with a thickness of the order of a few atomic layers [9]. Both of these band-gap engineering approaches have so far failed to produce quantum efficiencies comparable to what is done routinely with silicon quantum dots, especially at room temperature.

3 Bulk Silicon LEDs

Silicon LEDs with high power efficiencies have been demonstrated [3]. To reach this value, it is necessary to take several steps. First, one uses silicon

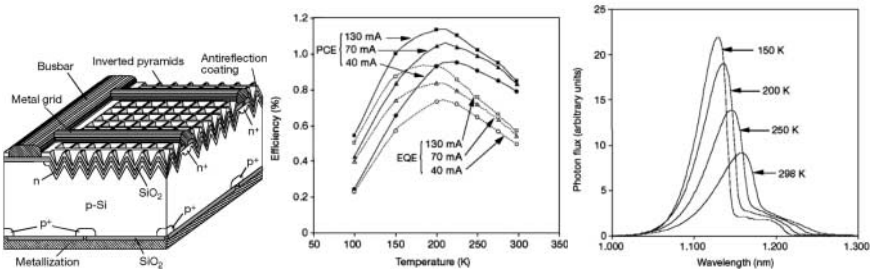

Fig. 6. (**a**) Schematic of a high-efficiency Si LED, showing the all the technological steps taken to maximize the efficiency, including the use of surface texturization. (**b**) Measured external quantum efficiency (EQE) and power efficiency (PCE) as a function of temperature for 3 current diodes. (**c**) Temperature dependence of the EL spectrum. After *Green* [3]

material with a long carrier lifetime indicative of a low defect density, such as wafers prepared by the float-zone method. Second, surface recombination is eliminated by using a high-quality surface oxide coating. Both of these steps increase η_{in}. Third, recombination and contact resistance are minimized by using small heavily-doped silicon/metal contact regions. This step increases η_{ext}. Fourth, the surface is textured in a way that is similar to the way the surface of highly efficient silicon solar cell is textured. Surface texturization improves the light extraction efficiency, thus minimizing the difference between η_{in} and η_{ext}. When these conditions are met, a power efficiency of 1% near room temperature has been demonstrated. Figure 6 shows how the surface of the LED is textured and the output spectrum and the efficiency versus temperature.

The advantage of this approach (compared to LEDs that use silicon quantum dots) is that electrical transport takes place in bulk silicon. Potential limitations of this approach can be summarized as follows. First, the maximum brightness of the device remains limited as the carrier lifetime is long and the injected carrier density must remain low enough to avoid Auger recombination. Second, direct modulation of the light output will be limited to speeds in the kHz regime as the carrier lifetime is long. Note that these two limitations are usually shared with all other monolithic silicon LEDs. Third, the requirements of high purity silicon, surface texturization, and relatively large device size make it difficult to integrate these LEDs into silicon microelectronic chips.

Another approach eliminates the need for high purity silicon. It consists of confining electrons and holes in small regions of space within the bulk silicon LED by introducing a strain field that locally modifies the band-gap [23]. This is achieved by introducing dislocation loops via ion implantation (boron

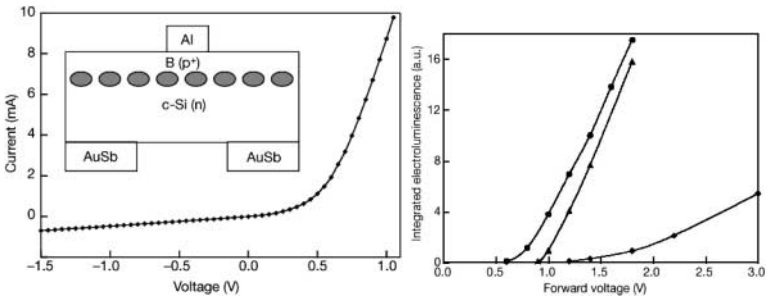

Fig. 7. Current-voltage characteristic and schematic of a Si LED containing dislocation loops in the active region. The integrated EL is plotted versus forward bias at three temperatures: from *left* to *right*, 300 K, 180 K, and 80 K. After *Ng* [23]

in n-type silicon) followed by thermal processing at 1000 °C in nitrogen. Each dislocation loop is tens of nm in size and calculations of the stress just outside the dislocation loop suggest that local band-gap around the loop can be increased by hundreds of meV [24]. This would be more than enough to confine the carriers inside the loop where they presumably will see no or very few defects and hence recombine efficiently at the silicon band-gap energy. Figure 7 shows the device cross-section and the dependence of the electroluminescence intensity on the forward voltage. Note that the EL spectra were similar to those of Fig. 6.

The advantage of this approach is that these LEDs can be fabricated using microelectronic-grade silicon. The potential limitations of this approach can be summarized as follows. First, the measured power efficiency is less 0.1% or less, although improvements would be expected with surface texturizing. Second, the brightness and modulation speeds are limited as in all monolithic Si LEDs. Third, an exact description of the microscopic phenomena is still lacking, and device-to-device reproducibility and device stability are not known.

4 Silicon Quantum Dot LEDs

Porous silicon containing silicon quantum dots has been widely used to make LEDs. Porous silicon is formed by the electrochemical dissolution of a silicon wafer (the anode) in a solution containing HF [25, 26]. When F^- and a hole injected from the wafer are both present at the interface, silicon dissolution takes place. If the current density is high or the HF concentration low, electropolishing takes place. Porous silicon is obtained by decreasing the current density or increasing the HF concentration such that the holes are the limiting species at the interface. The size of the pores and the silicon remnants can be tuned from the nanometer regime to beyond 1 μm [27]. Light emission is especially strong in "spongy" porous silicon that contains typical feature sizes in the nanometer range [28, 29]. Figure 8 shows the strong

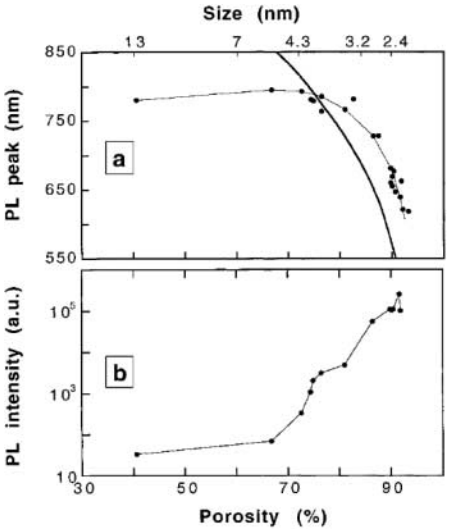

Fig. 8. Measured PL peak wavelength and PL intensity on various oxidized porous silicon films (the *full line* in graph a is a theoretical prediction). The porosity was measured gravimetrically and the average quantum dot size determined by Raman spectroscopy. The PL peak is in broad agreement with the results shown in Fig. 4 except for sizes above ~ 4.5 nm when Pl is due to defects inside the oxide. The PL peak intensity increases by several orders of magnitude as the average size decreases to ~ 2.5 nm. After *Fauchet* [30]

increase in PL efficiency as the porosity increases/average quantum dot size decreases [30]. Porous silicon is naturally passivated by Si-H bonds. While these bonds provide excellent surface passivation, they are very fragile and susceptible to dissociation by many external stimuli such as heat or UV light exposure. Surface treatments such as oxidation [31] or formation of silicon-carbon bonds [32] improve the stability of the optical properties.

After the first demonstration of porous silicon LEDs, the power efficiency was quickly improved to $\sim 0.01\%$ [33]. This progress was made possible by better control of the materials science, especially the stability of silicon surface, and by improved device engineering to decrease the problems associated with charge transport in porous silicon and with the interface between porous silicon and a metal contact. After additional device optimization, power efficiencies in the 0.1% range were reported and stability in excess of 100 h was achieved [31,34]. It remained to be shown that porous silicon LEDs could be fabricated and integrated with silicon microelectronic circuitry. Integration of a porous silicon LED with a transistor was first reported in 1996 [35]. Figure 9 shows the device structure and its stability.

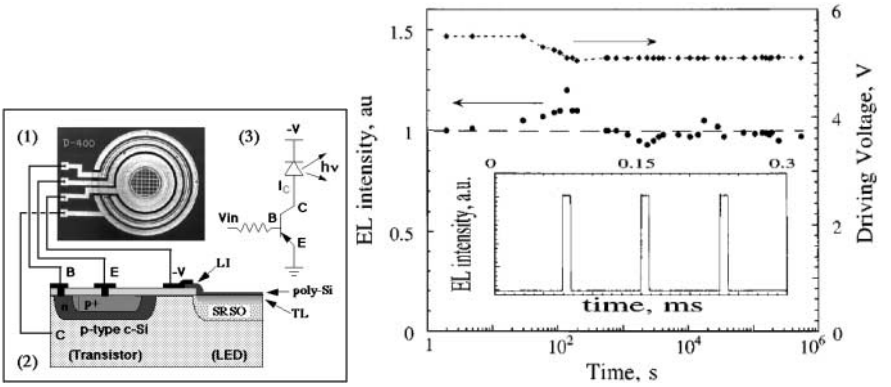

Fig. 9. Top-view picture, cross-sectional schematic, and equivalent circuit representation of a porous silicon LED integrated with a pnp transistor. The electroluminescence of a similar LED showed no degradation over days of operation under pulsed operation. After *Hirschman* [35] and *Tsybeskov* [31]

The major problems specific to porous silicon LEDs are the long-term stability, the achievable power efficiency, and the broad emission spectrum. Let us consider recent progress in each of these areas.

Steady work has continued to increase the efficiency. The external quantum efficiency of these devices was first brought up close to 1% but because the LEDs required high applied voltages ($> 10\,\mathrm{V}$), the power efficiency was still $\sim 0.1\%$ [36] With better device engineering power efficiencies very close to 1% have been achieved [37]. An important requirement for high efficiency is to keep the thickness of the porous layer to 1 μm or less. How the external quantum efficiency can be further increased remains a research topic.

In the early porous silicon LED work, little attention was paid to the passivation of the internal surface. Hence, the stability of the devices was poor. Significant progress was achieved via oxidation but the price to be paid is that transport is made more difficult as oxide barriers may be introduced. Alternative surface stabilization techniques based on silicon-carbon and silicon-carbon-oxygen bonds have been developed [38] and used to produce stable LEDs [39]. It will be interesting to see if this approach can also lead to higher efficiencies and if these LEDs can be integrated successfully with microelectronic fabrication technology.

The PL and EL spectrum of all samples containing silicon quantum dots, including porous silicon, is broad. The spectral width can be due to the quantum dot size distribution but it may also arise from the intrinsically broad luminescence linewidth of small silicon quantum dots [40, 41]. For many applications, a narrow linewidth is necessary. This can be achieved by using a microcavity. The porosity can be controlled over a wide range by changing several parameters during etching, especially the current density. Since etching requires holes at the Si/electrolyte interface and transport of holes

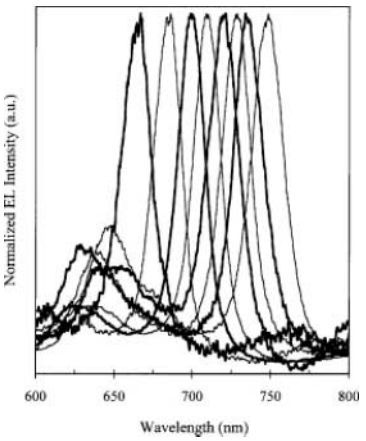

Fig. 10. Electroluminescence spectra measured with 8 porous silicon microcavity LEDs consisting of a thin light-emitting layer sandwiched between two Bragg reflectors. The porosity of the active layer and hence its refractive index was changed to achieve tuning over a 100 nm range. After *Chan* [44]

from the silicon wafer into the porous layer is preferentially to the pore tips, the properties of an existing porous layer are unaffected by further etching. Layers of different porosities can be produced by changing the current density during etching. This approach has led to anti-reflection coatings [13], Braggreflectors [42], and microcavities [43]. Microcavity LEDs made of a high porosity, light emitting layer sandwiched between two porous Braggreflectors have been demonstrated. Their EL spectra are shown in Fig. 10 [44]. Note that the PL spectrum of porous silicon microcavities can be narrowed to below 1 nm [45,46]. The LEDs can be made to cover a large region of wavelengths by simply changing the porosity and/or the thickness of the layers. They are tunable in the same sense as $Al_xGa_{1-x}As$ LEDs are tunable (changing the alloy content is equivalent to changing the porosity or the layer's thickness). The main limitation of this approach is that the power efficiency of these microcavities is very low because charge transport over several microns of porous silicon is difficult.

There are many methods to produce silicon quantum dots and all of them can lead to efficient PL [47]. Two of the most popular approaches besides porous silicon are annealing of silicon-rich SiO_2 and annealing of amorphous Si/SiO_2 superlattices. Silicon-rich SiO_2 films can be produced by implantation of SiO_2 with high doses of silicon ions or by directly depositing a substoichiometric oxide for example by plasma enhanced chemical vapor deposition. In both cases, annealing at high temperature (typically 1000 °C) is required to form silicon clusters, crystallize them, and passivate them. There are many similarities between annealed silicon-rich SiO_2 and porous silicon. The average size of the silicon quantum dots can be varied from $\sim$ 2 nm

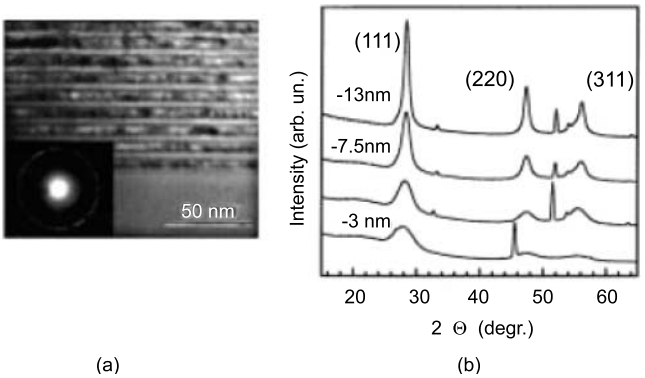

Fig. 11. Cross-sectional TEM picture of an annealed and crystallized a-Si/SiO_2 superlattice. The SiO_2layers appear as the continuous *bright* layers, while the crystallized silicon layers contain *bright* and *dark* spots, corresponding to quantum dots of various orientations. The X-ray data shown on the *right*, taken on similar structures with different thicknesses of the Si layers, confirms the formation of quantum dots whose sizes are given by the thickness of the a-Si layers. After *Tsybeskov* [48]

to sizes where quantum confinement stops being important. The quantum dots are produced with a range of sizes characterized by a standard deviation that is 20% to 50% of the average. In contrast, annealing of amorphous Si/SiO_2 superlattices grown by techniques such as sputtering produces multiple layers made of a densely-packed array of silicon quantum dots whose diameters are uniform, equal to the thickness of the a-Si layers [48, 49]. Figure 11 shows a typical structure. By substituting non-stoichiometric oxide for the a-Si layer, it is possible to increase the dot-to-dot separation in each layer of these nanocrystalline Si superlattices [50].

LEDs have been made using either annealed silicon-rich SiO_2 [51, 52] or nanocrystalline Si superlattices (with CaF_2) [53]. Figure 12 shows the room temperature EL spectrum and the dependence of the EL intensity on applied voltage for an MOS-like device with a very thin (25 nm) silicon-rich SiO_2 layer [54]. To achieve threshold for electroluminescence at a voltage as low as ~ 4 V, the thickness of the silicon-rich SiO_2 must remain very small (much less than 100 nm) and the distance between adjacent silicon quantum dots small enough to allow reasonable charge transport under bias. Limitations with this approach include the low brightness achievable (due to the thin light-emitting layer) and the relatively high leakage current (due to the high density of quantum dots). In addition, direct modulation is limited to low frequencies as in all monolithic Si LEDs.

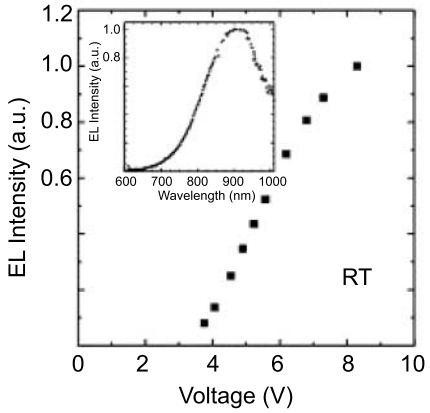

Fig. 12. Room-temperature electroluminescence intensity versus forward bias for an LED where the active layer is a 25 nm thick silicon-rich oxide layer annealed to produce ~ 2 nm silicon quantum dots embedded in SiO_2. The *inset* shows the EL spectra measured at 4 V with a current density of 0.4 mA/cm^2. After *Irrera* [52]

5 SiGe LEDs

Bandgap engineering of III–V semiconductor structures started 30 years ago and today many commercial devices exist that use this approach. These include LEDs and lasers. It is thus reasonable to expect that band-gap engineering involving elements of the 4$^{\text{th}}$ column of the periodic table would produce useful devices, including light sources. The SiGe alloy system is by far the most studied system [9]. Because of the large ($\sim 4\%$) lattice mismatch between Si and Ge, it is not possible to grow thick layers of Ge on Si without introducing dislocations. The strain present in SiGe structures is thus a limitation that does not exist in many III–V semiconductor systems. It can also be thought of as an additional degree of freedom as various degrees of strain can change the band-gap.

SiGe layers can be grown by molecular beam epitaxy [54] or low-pressure chemical vapor deposition [55]. strain in the active layers can be managed through the use of a thick alloy layer grown directly on the silicon substrate. This thick layer is relaxed and thus subsequent layers grown on it respond to the natural lattice constant of the relaxed layer, not that of the Si substrate. However, by using small growth areas, it is possible to grow thicker SiGe layers that remain strained and do not contain dislocations [56].

SiGe LEDs have been demonstrated using Si_nGe_m multilayers, SiGe quantum wells, and thick SiGe layers. Figure 13 shows the EL spectrum of devices in which the light is emitted by a thick SiGe layer [57]. All SiGe LEDs suffer from the same strong decrease in efficiency with increasing temperature. In fact, the best SiGe LEDs have a power efficiency that is at least one order of magnitude below that of good Si LEDs. Two main reasons explain this

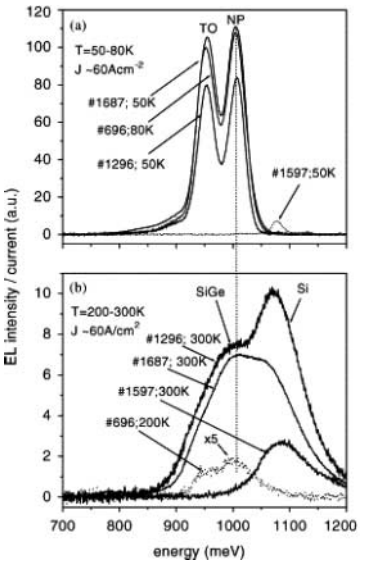

Fig. 13. Measured low-temperature and high-temperature electroluminescence spectra for LEDs in which the active layer is a strained SiGe layer. The thickness of this layer is 60 nm, 260 nm, and 445 nm in samples 696, 1296, and 1687 respectively. At low temperature, two peaks are measured, corresponding to recombination without phonon participation (NP) and with phonon participation (TO). At high temperature, the *lines* broaden and emission is also measured in silicon, as confimed by the measurement performed on a Si LED (sample 1597). After *Stoica* [57]

low efficiency. First, SiGe is still an indirect gap semiconductor, making it imperative to eliminate non-radiative centers. Second, the small band-gap discontinuity between SiGe and Si (compared to that between Si and SiO_2 for example) makes it difficult to prevent the carriers from escaping the active layer.

Recently, the activity in this material system has moved to emission from Ge islands or quantum dots [58,59] and to quantum cascade lasers that involve intraband transitions [60, 61]. The first approach is related to the on-going work on III–V semiconductor quantum dot laser and electroluminescence is only starting to emerge. The second approach does not involve transitions across the fundamental band-gap, leads to light emission in the mid to far infrared, and is thus beyond the scope of this chapter.

6 Erbium-doped Silicon LEDs

Specific light-emitting centers can be introduced into silicon. In this case, silicon itself is not directly involved in the light emission but rather serves as

a host in which charge carriers are produced. These charges then are transferred to the light-emitting centers that produce sub-band-gap luminescence. This section focuses on erbium as the luminescent center, as it appears to be the most promising choice.

Erbium is widely used as a light source at the important optical wavelength of 1.54 μm. Emission at this wavelength is due to an intra-center transition between level $^4I_{13/2}$ and level $^4I_{15/2}$. The radiative lifetime is long ($\sim$ ms) and the oscillator strength of the transition is weak, not unlike in silicon itself. In silica optical fibers, erbium-doped amplifiers are used to periodically boost the optical signal. These amplifiers are long because of the weak transition rate and because the maximum density of erbium atoms is limited in order to avoid clustering of the erbium atoms that would quench the light emission.

Luminescence at 1.5 μm was first achieved in erbium-doped bulk silicon [62]. LEDs were then demonstrated and efficiencies up to near 0.1% achieved at room temperature [63]. In these devices, it is desirable that the Er ions be excited by impact excitation. It is unlikely that the performance of erbium-doped bulk Si LEDs can be improved for the following fundamental reasons: the limited maximum energy of hot electrons in silicon, efficient energy losses such as Auger recombination with free carriers in silicon or energy back transfer [64], and the limited maximum density of Er atoms to avoid clustering. At least a partial solution to these problems has been made possible by using silicon quantum dots embedded in SiO_2 instead of bulk silicon. The larger band-gap of silicon quantum dots minimizes energy back transfer to Si from Er. The use of the SiO_2 matrix guarantees that there are no free carriers that can participate in Auger recombination. More than one active Er can be excited per nanocrystal leading to a large concentration of active Er centers. Since transport takes place in an oxide matrix containing silicon quantum dots, efficient LEDs require a thin oxide layer and a large concentration of silicon quantum dots.

Figure 14 shows the cross-section of an Er-doped LED. It is an MOS structure in which the Er atoms (and the silicon quantum dots) are in the thin oxide layer. Figure 14 also shows the room temperature EL spectrum of a device that does not contain silicon quantum dots (i.e., contains a stoichiometric oxide) together with a plot of the emitted optical power as a function of the drive current [65]. Even in the absence of silicon quantum dots, the optical output of the LED is comparable to that of a III–V semiconductor LED. However, because the current-voltage curves indicate that transport takes place in the Fowler–Nordheim regime, wearout of the oxide is significant and the voltage needed to achieve a given current is very high, which limits the power efficiency. Figure 15 shows the EL spectra for a related device containing silicon quantum dots only and silicon quantum dots with erbium [66]. At low injection current density, the efficiency of the devices with and without erbium is comparable. The reported external quantum efficiency

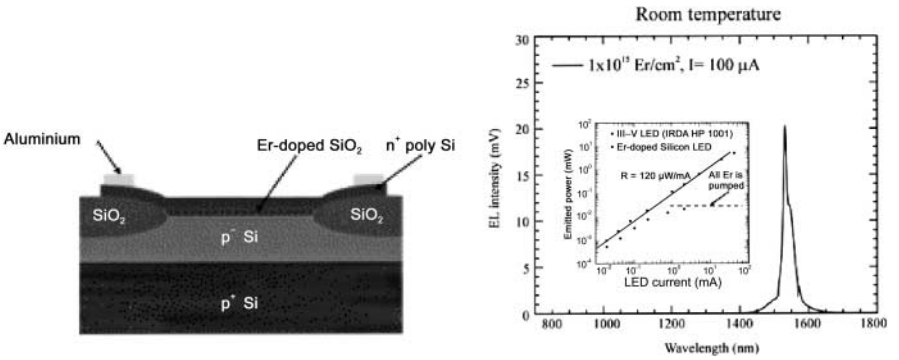

Fig. 14. Schematic cross-section of an MOS-like LED in which light emission takes place in a 70-nm-thick erbium-doped SiO_2 or silicon-rich SiO_2 layer. Measured room-temperature electroluminescence intensity spectrum for a stoichiometric oxide. The *inset* shows how the EL power increases with current. Until all the erbium atoms are pumped, this Si-based LED is comparable to a commercial III–V semiconductor LED. After *Castagna* [65]

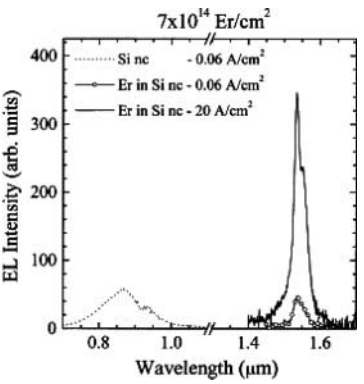

Fig. 15. Room-temperature electroluminescence spectra for an MOS-like Si LED that contain a 200-nm-thick silicon-rich SiO_2 layer. The average quantum dot size is 3.4 nm. Samples without Er showed weak EL in the near infrared whereas samples doped with erbium ($6.5 \times 10^{20}\,\mathrm{cm}^{-3}$) showed strong EL near 1.5 μm. After *Pacifici* [66]

of some of the Er-doped LEDs is 10% or greater [65] and it is anticipated that the power efficiency of these devices will be able to make them commercially viable. Note that using the same approach EL from other rare earths such as ytterbium and terbium has been achieved [65].

The advantages of erbium-doped LEDs include the emission wavelength (1.5 μm light is not absorbed by silicon) and the record efficiencies that make them competitive with III–V semiconductor LEDs. Their potential limita-

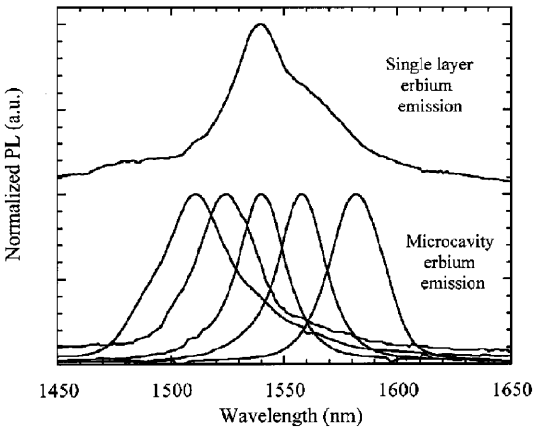

Fig. 16. Measured photoluminescence spectrum in an erbium-doped oxidized porous silicon film and measured spectra when the layer is embedded in different microcavities. After *Lopez* [67]

tions are the long-term stability of the devices and the limited speed of operation.

The luminescence spectrum of erbium-doped silicon is much narrower than that produced by silicon quantum dots. However, the emission is not really monochromatic. As mentioned earlier, the luminescence linewidth from a material can be narrowed by inserting the light emitting layer inside a microcavity. This has also been accomplished with erbium-doped porous silicon [67]. Figure 16 shows tuning of the luminescence near 1.5 μm for porous silicon microcavities doped with erbium. Because the thickness of the entire microcavity makes charge transport very inefficient [68], the achievable efficiencies of microcavity LEDs would make them unacceptable, unless an alternate electrical pumping method can be demonstrated.

7 Prospects for a Silicon-based Laser

Could a silicon laser ever be made? And if it can be made, can it be pumped electrically and can it become efficient enough to be put in use? These questions were not even raised until 2000 and yet the situation has changed drastically ever since. Entire conferences have even been devoted to the topic [69]. There are several fundamental differences between a laser and an LED. The output of a laser is coherent, of tentimes narrow band and directional. Unlike an LED, a laser is capable of producing short pulses whose duration is not related to the radiative lifetime. Thus a silicon laser could circumvent most of the limitations associated with silicon LEDs.

To achieve lasing, one first needs to achieve population inversion. In practice, this means that the upper lasing level is rapidly filled from some higher-

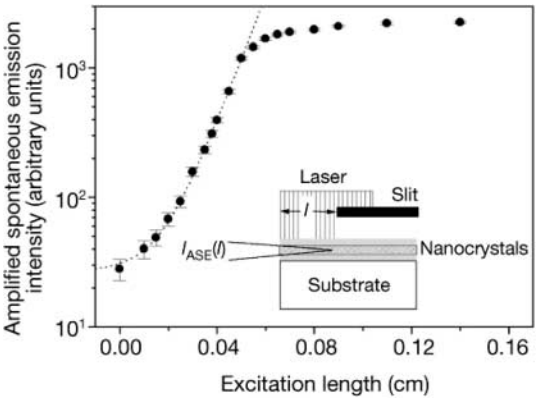

Fig. 17. Exponential growth of the amplified spontaneous emission measured by the variable stripe length method (see *inset*) on a sample containing silicon quantum dots embedded in a SiO_2 layer. The exponential growth is indicative of gain as the signal should increase as $\exp gl$, where l is the excitation length and g is the gain coefficient. After *Pavesi* [70]

lying level, and the lower lasing level is rapidly depleted of its population to some lower-lying level. This is very hard, if not impossible, to achieve in bulk silicon, where excited state absorption (i.e., free carrier absorption) and Auger recombination compete with stimulated emission. In silicon quantum dots however, the situation may become different. The radiative recombination rate increases and while pumping may involve silicon quantum dot states, lasing may involve surface states, which makes it easier to achieve population inversion. Lasing also requires that the achievable optical gain exceeds the losses associated with the cavity (i.e., mirror reflectivity, absorption losses, scattering losses).

Observations of optical gain have made using a single-pass amplifier geometry in different samples containing silicon quantum dots [70,71,72]. Figure 17 shows results from the first publication on this topic [70]. An exponential growth of the signal is observed under constant optical pumping intensity as the pumping length increases, in agreement with expectations for optical gain. Figure 18 shows that as the pumping intensity is increased, switching from losses to gain is observed [72]. In these experiments, gain was observed only under pulsed pumping and not cw excitation, presumably because pulsed excitation produces a larger density of photoinjected carriers. The origin of the gain and even its existence are still under debate. It appears unlikely that gain involves recombination of an electron and a hole within silicon quantum dots. Silicon-oxygen bonds may be involved but presently there is no confirmation of this. Other experiments have also failed to exhibit gain [73] casting doubt on the existence of gain itself.

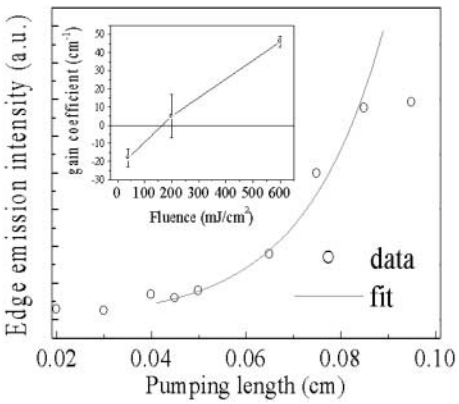

Fig. 18. Exponential growth of the amplified spontaneous signal measured using the variable stripe length method on a crystallized Si/SiO_2 superlattice similar to that in Fig. 11. The *inset* shows how the behavior can switch from loss to gain when the pump laser fluence increases. After *Ruan* [72]

These uncertainties should be settled after more focused work. The real test is whether a laser cavity can be build and lasing achieved. Once a laser is demonstrated, it will be possible to measure and optimize the performance of a silicon-based laser and to evaluate whether such a laser can have attractive properties and become viable. The major potential obstacle to the realization of a practical silicon-based laser is the need to pump it electrically, not optically. As we have already seen in other sections, electrical pumping is very often much less efficient than optical pumping, raising the prospect that lasing threshold may not be achievable. Note that erbium-doped samples also appear to be attractive candidates for achieving lasing.

Acknowledgements

Work in the author's laboratory related to silicon light sources has been supported in part by the National Science Foundation, the Army Research Office, and the Semiconductor Research Corporation. Contributions from the following present and past group members are gratefully acknowledged: Selena Chan, Hui Chen, Karl Hirschman, Herman Lopez, Cheng Peng, Jinhao Ruan, Leonid Tsybeskov, and Michal Wolkin.

References

1. I. Schnitzer, E. Yablonovitch, C. Caneau, T. J. Gittmer: Appl. Phys. Lett. **62**, 131–133 (1993)
2. E. Yablonovitch, D. L. Allara, C. C. Chang, T.J. Gmitter, T. B. Bright: Phys. Rev. Lett. **57**, 249 (1986)

3. M. A. Green, J. Zhao, A. Wang, P. J. Reece, M. Gal: Nature **412**, 805–808 (2001)
4. E. Yablonovitch, T. Gmitter: Appl. Phys. Lett. **49**, 587 (1986)
5. M. S. Hybertsen: Phys. Rev. Lett. **72**, 1514 (1994)
6. T. G. Brown, D. G. Hall: in *Light Emission in Silicon: From Physics to Devices*, ed. by D. J. Lockwood, Semicond. Semimet. **49** (Academic Press, San Diego 1997), chap. 3
7. G. Abstreiter: Phys. World **5**, 36 (1992)
8. B. A. Orner, J. Olowolafe, K. Roe, J. Kolodzey, T. Laursen, J. W. Mayer, J. Spear: Appl. Phys. Lett. **69**, 2557 (1996)
9. G. Abstreiter: In: *Light Emission in Silicon: From Physics to Devices*, ed. by D. J. Lockwood, Semicond. Semimet. **49** (Academic Press, San Diego 1997), chap. 2
10. J. Michel, L. V. C. Assali, M. T. Morse, L. C. Kimerling: In: *Light Emission in Silicon: From Physics to Devices*, ed. by D. J. Lockwood, Semicond. Semimet. **49** (Academic Press, San Diego 1997), chap. 4
11. S. Lombardo, S. U. Campisano, G. N. van den Hoven, A. Cacciato, A. Polman: Appl. Phys. Lett. **63**, 1942 (1993)
12. J. Gowar: *Optical Communication Systems* (Prentice-Hall, London 1984), p. 245
13. C. C. Striemer, P. M. Fauchet: Appl. Phys. Lett. **81**, 2980 (2002)
14. M. L. Cohen, J. Chelikowsky: *Electronic Structure and Optical Properties of Semiconductors*, 2nd edn. (Springer, Berlin 1989)
15. G. Davies: Phys. Rep. **176**, 83 (1989)
16. C. Delerue, G. Allan, M. Lannoo: In: *Light Emission in Silicon: From Physics to Devices*, ed. by D. J. Lockwood, Semicond. Semimet. **49** (Academic Press, San Diego 1997), chap. 7
17. C. Delerue, G. Allan, M. Lannoo: J. Lumin. **80**, 65 (1999)
18. M. Wolkin, J. Jorne, P. M. Fauchet, G. Allan, C. Delerue: Phys. Rev. Lett. **82**, 197 (1999)
19. M. Luppi, S. Ossicini: J. Appl. Phys. **94**, 2130 (2003)
20. W. Jantsch, S. Lanzerstorfer, L. Palmetshofer, M. Stepikhova, H. Preier: J. Lumin. **80**, 9 (1999)
21. G. Franzo, F. Priolo, S. Coffa: J. Lumin. **80**, 19 (1999)
22. T. P. Pearsall: Prog. Quant. Opt. **18**, 97 (1994)
23. W. L. Ng, M. A. Lourenco, R. M. Gwilliam, S. Ledain, G. Shao, K. P. Homewood: Nature **410**, 192–194 (2001)
24. M. A. Lourenco, M. S. A. Siddiqui, G. Shao, R. M. Gwilliam, K. P. Homewood: In: *Towards the First Silicon Laser*, ed. by L. Pavesi, S. Gaponenko, L. Dal Negro, NATO Science Series (Kluwer Academic, Dordrecht 2003), pp.11–20
25. R. L. Smith, S. D. Collins: J. Appl. Phys. **71**, R1 (1992)
26. A. G. Cullis, L. T. Canham, P. D. J. Calcott: J. Appl. Phys. **82**, 909 (1997)
27. L. T. Canham (Ed.): *Properties of Porous Silicon*, Electronic Materials Information Service Datareviews Series **18** (INSPEC, The Institution of Electrical Engineers, London 1997)
28. R. T. Collins, M. A. Tischler, P. M. Fauchet: Physics Today **50**, 24 (1997)
29. P. M. Fauchet: In: *Light Emission in Silicon: From Physics to Devices*, ed. by D. J. Lockwood, Semicond. Semimet. **49** (Academic Press, San Diego 1997), chap. 6

30. P. M. Fauchet, J. von Behren: Phys. Stat. Sol. (b) **204**, R7 (1997)
31. L. Tsybeskov, S. P. Duttagupta, K. D. Hirschman, P. M. Fauchet: Appl. Phys. Lett. **68**, 2058 (1996)
32. J. M. Buriak, M. J. Allen: J. Lumin. **80**, 29 (1999)
33. W. Lang, P. Steiner, F. Kozlowski: J. Lumin. **57**, 341 (1993)
34. A. Loni, A. J. Simmons, T. I. Cox, P. D. J. Calcott, L. T. Canham: Electron. Lett. **31**, 1288 (1995)
35. K. D. Hirschman, L. Tsybeskov, S. P. Duttagupta, P. M. Fauchet: Nature **384**, 338 (1996)
36. K. Nishimura, Y. Nagao, N. Ikeda: Jpn. J. Appl. Phys. **37**, L303 (1998)
37. B. Gelloz, N. Koshida: J. Appl. Phys. **88**, 4319–4324 (2000)
38. J. M. Buriak, M. J. Allen: J. Am. Chem. Soc. **120**, 1339 (1998)
39. B. Gelloz, H. Sano, R. Boukherroub, D. D. M. Wayner, D. J. Lockwood, N. Koshida: Appl. Phys. Lett. **83**, 2342–2344 (2003)
40. J. Valenta, R. Juhasz, J. Linnros: Appl. Phys. Lett. **80**, 1070 (2002)
41. C. Delerue, G. Allan, M. Lannoo. Phys. Rev. B **64**, 193402 (2001)
42. M. G. Berger, C. Dieker, M. Thonissen, L. Vescan, H. Luth, H. Munder, W. Theiss, M. Wernke, P. Grosse: J. Phys. D: Appl. Phys. **27**, 1333 (1994)
43. L. Pavesi: La Rivista del Nuovo Cimento **20**, 1 (1997)
44. S. Chan, P. M. Fauchet: Appl. Phys. Lett. **75**, 274 (1999)
45. P. J. Reece, G. Lerondel, W. H. Zheng, M. Gal: Appl. Phys. Lett. **81**, 4895 (2002)
46. M. Ghulinyan, C. J. Oton, G. Bonetti, Z. Gaburro, L. Pavesi: J. Appl. Phys. **93**, 9724 (2003)
47. P. M. Fauchet: J. Lumin. **70**, 294 (1996)
48. L. Tsybeskov, K. D. Hirschman, S. P. Duttagupta, M. Zacharias, P. M. Fauchet, J. McCaffrey, D. J. Lockwood: Appl. Phys. Lett. **72**, 43 (1998)
49. G. F. Grom, D. J. Lockwood, J. P. McCaffrey, H. J. Labbe, P. M. Fauchet, B. White, Jr., J. Diener, D. Kovalev, F. Koch, L. Tsybeskov: Nature **407**, 358 (2000)
50. M. Zacharias, J. Heitmann, R. Scholz, U. Kahler, M. Schmidt, J. Blasing: Appl. Phys. Lett. **80**, 661 (2002)
51. N. Lalic, J. Linnros: J. Lumin. **80**, 263 (1999)
52. A. Irrera, D. Pacifici, M. Miritello, G. Franzo, F. Priolo, F. Iacona, D. Sanfilippo, G. Di Stefano, P. G. Fallica: Physica E **16**, 395 (2003)
53. V. Ioannou-Sougleridis, A. G. Nassiopoulou, T. Ouisse, F. Bassani, F. A. d'Avitaya: Appl. Phys. Lett. **79**, 2076 (2001)
54. G. Abstreiter, K. Eberl, E. Friess, W. Wegscheider, R. Zachai: J. Cryst. Growth **95**, 431 (1989)
55. T. Stoica, L. Vescan, M. Goryll: J. Appl. Phys. **83**, 3367 (1998)
56. L. Vescan, T. Stoica: J. Lumin. **80**, 485 (1999)
57. T. Stoica, L. Vescan, A. Muck, B. Hollander, G. Schope: Physica E **16**, 359 (2003)
58. A. Beyer, E. Muller, H. Sigg, S. Stutz, D. Grutzmacher: Appl. Phys. Lett. **77**, 3218 (2000)
59. N. N. Ledentsov: In: *Towards the First Silicon Laser*, ed. by L. Pavesi, S. Gaponenko, L. Dal Negro, NATO Science Series (Kluwer Academic, Dordrecht 2003) pp. 281–292

60. D. J.Paul, S. A. Lynch, R. Bates, Z. Ikonic, R. W. Kensall, P. Harrison, D. J. Norris, S. L. Liew, A. G. Cullis, P.Murzyn, C.Pidgeon, D. D. Arnone, D. J. Robbins: Physica E **16**, 309–314 (2003)
61. L. Diehl et al.: Physica E **16**, 315 (2003)
62. H. Ennen, J. Schneider, G. Pomrenke, A. Axmann: Appl. Phys. Lett. **43**, 943 (1983)
63. G. Franzo, F. Priolo, S. Coffa, A. Polman, A. Carnera: Appl. Phys. Lett. **64**, 2235 (1994)
64. G. Franzo, F. Priolo, S. Coffa, A. Carnera: Phys. Rev. B **57**, 4443 (1998)
65. M. E. Castagna, S. Coffa, M. Monaco, L. Caristia, A. Messina, R. Mangano, C. Bongiorno: Physica E **16**, 547 (2003)
66. D. Pacifici, A. Irrera, G. Franzo, M. Miritello, F. Iacona, F. Priolo: Physica E **16**, 331 (2003)
67. H. A. Lopez, P. M. Fauchet: Appl. Phys. Lett. **77**, 3704 (2000)
68. H. A. Lopez, P. M. Fauchet: Mat. Sci. Eng. B **81**, 91 (2001)
69. L. Pavesi, S. Gaponenko, L. Dal Negro (Eds.): *Towards the First Silicon Laser* (Kluwer, Dordrecht 2003)
70. L. Pavesi, L. Dal Negro, C. Mazzoleni, G. Franzo, F. Priolo: Nature **408**, 440 (2000)
71. L. Khriachtchev, M. Rasanen, S. Novikov, J. Sinkkonen: Appl. Phys. Lett. **79**, 1249 (2001)
72. J. Ruan, P. M. Fauchet, L. Dal Negro, M. Cazzanelli, L. Pavesi: Appl. Phys. Lett. **83**, 5479 (2003).
73. R. G. Elliman, M. J. Lederer, N. Smith, B. Luther-Davies: Nucl. Instr. Meth. B **206**, 427 (2003)

Index